Flight Evaluation of the Characteristics of a Variable Span Wing

Joaquim Sousa

Aerospace Sciences Department
Universidade da Beira Interior
6200-254 Covilhã, Portugal

Abstract

This paper describes the work done on the instrumentation and flight testing of an Unmanned Aerial Vehicle (UAV) in order to evaluate its aerodynamic performance in flight. The UAV, called Olharapo, was developed in previous works at the Department of Aerospace Sciences of University of Beira Interior and it has two configurations: it can be fitted with a conventional fixed wing or a variable span morphing wing (VSW). With the aim of determining the performance of the UAV with these wings fitted, several systems such as a First Person View (FPV) system, a long range radio control system and an autopilot system were integrated and incorporated. These systems allow the acquisition of the essential data for performance determination and also permit real time control and communications. Numerous flight tests were conducted and a curve of aerodynamic efficiency for the conventional fixed wing was obtained. For the VSW, three different wingspan configurations were tested: a full wingspan configuration of 2.5m, an intermediate configuration of 2m and a minimum wingspan configuration of 1.5m. For this wing it was not possible to achieve a well defined curve of efficiency for each wingspan configuration due to insufficient data, thus, more flight tests should be conducted to completely characterize the aerodynamic efficiency of the VSW.

Key words: UAV, Morphing Wing, Variable Span, Instrumentation, Autopilot, FPV, Flight tests, Aerodynamic Efficiency

1. Introduction

In the past years the development of morphing wing technologies has been a matter of great interest from the scientific community. These technologies potentially enable an increase in aircraft efficiency by changing the wing shape thus allowing the aircraft to fly near its optimal performance point. Tidwell et al [1] clearly demonstrated the advantages of these technologies where the flight envelope of a fixed geometry aircraft can be expanded so that new multi-role missions could be performed.

These technologies can be divided into three different categories according to the type of geometric transformation: out-of-plane transformations, airfoil adjustments and planform alterations. The out-of-plane transformations include twist, dihedral and span-wise bending. Regarding airfoil adjustments the camber and thickness are the main geometric transformations. Finally, the planform alterations include a variation on the wing's chord, sweep and span. Regarding the wing span variation several concepts have been developed [2-11]. The very first concept of this morphing wing technology was developed by Ivan Makhonine on the MAK-10. This aircraft had a telescopic mechanism where the outer panels of the wing slide in inside the wing's centre panels [12]. Alongside morphing technologies, the development of unmanned aerial vehicles (UAV) has undergone a major expansion in recent years. These vehicles are an excellent platform for testing new concepts of morphing wings. The use of UAVs for testing new concepts presents numerous advantages such as low production cost, no flight crew is required and since they are subjected to low aerodynamic loads the use of several morphing technologies are potentiated [13].

The work described in this paper deals with instrumenting and flight testing the Olharapo UAV in order to evaluate its aerodynamic performance in flight. This UAV has two configurations: one with a fixed wing and another with a variable span morphing wing.

2. UAV description

The Olharapo UAV is a result of previous works developed at Department of Aerospace Sciences of University of Beira Interior. This UAV can be fitted with different wings thus making a good platform for wing testing.

2.1. Airframe description

This UAV is a high-wing pusher with the particularity of having the propeller behind the H tail. In previous versions this UAV had a V tail which was then replaced by an H tail that is capable of maneuvering the UAV without the need of using ailerons. This tail replacement can be seen as a safety measure for testing the VSW. The fuselage is made out of carbon/epoxy composite and wood. The conventional fixed wing is made of balsa wood ribs, a hard wood main spar and a balsa wood torsion box. This wing has a wingspan of 2.5m and the wing's chord is 0.25m. The airfoil used on this wing is a SG6042 which is a low speed airfoil with a good compromise between maximum lift coefficient, efficiency and thickness. This aircraft was designed to fly in a speed range from 11m/s to 40m/s.

2.2. Development of the variable span wing (VSW)

The development of the VSW began with an aerodynamic shape optimization that was used to determine the optimal values of wing span for the speed range of the vehicle's flight envelope[14]. The roll rate available with asymmetric span control of the VSW was analyzed. This analysis showed that roll control authority exists over the required speed range, where the roll motion can be achieved by asymmetric wing extension of the VSW[15].. This wing does not exhibit any dihedral or any sweep and is made of one rectangular inboard part (inner fixed wing – IFW) with a chord of 0.265m and a rectangular outboard part (outer moving wing – OMW) with a chord of 0.245m. The airfoil used in this wing is a modified SG6042. The telescopic mechanism consists on a hollow wing (IFW) inside of which a smaller conventional wing slides (OMW) actuated by a simple electromechanical rack and pinion mechanism. The pinion is driven by a servomotor installed at the center of the wing assembly and pushes/pull the rack that is attached to the OMW. A full scale prototype was built [16]. A structural design and analysis using a FEM model were developed to analyze the VSW structure. The wing was also subjected to bench tests where the experimental results showed to be in agreement with the numerical simulations. From this study it was observed that the wing structure is able to support the extensions and forces due to aerodynamics loads within the flight enveloped defined (11m/s to 40m/s)[17]. An aeroelastic analysis using the typical aeroelastic section with unsteady linearized potential theory together with the aerodynamic strip theory was also performed to determine the critical flutter speed. From this study, it was concluded that the critical flutter speed was significantly higher than the maximum speed of the flight envelope, allowing the aircraft to safely fly within the defined range of speeds[18].

In figure 1a) it is possible to see the actuation mechanism of the VSW and in figure 1b) the actual Olharapo UAV fitted with the variable span wing.

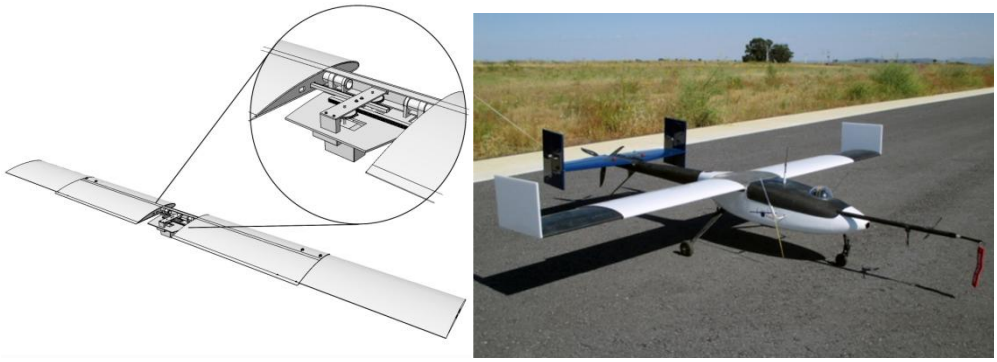

Figure 1 - a) Telescopic wing mechanism b) Olharapo UAV fitted with telescopic wing.

3. Flight testing

The main objective of flight testing is to acquire the flight data that allows the aerodynamic efficiency to be determined. For that purpose, several systems such as a FPV system, a long range radio control system and an autopilot system were incorporated in the UAV. To safely validate the integration of these systems, an off-the-shelf UAV called Skywalker was used [19]. After several flight tests with this RC model, all the systems proved to work properly, allowing their installation on the Olharapo UAV.

3.1. Lift-to-drag ratio determination

Prior to conducting the flight tests, it was necessary to analyze the flight mechanics of the vehicle to determine under what conditions the flight should be conducted. In a simple manner, considering the propulsive force of the aircraft is unknown, one can perform gliding flights where this force is zero. Through the analysis of flight mechanics it was possible to obtain three different methods for calculating the lift-to-drag ratio.

In gliding conditions the only forces to balance the weight are lift (*L*) and drag (*D*) that are given by the following equations:

$$D = W.\sin(\gamma) \tag{1}$$

$$L = W.\cos(\gamma) \tag{2}$$

In the first method, the aerodynamic efficiency (*E*) or lift-to-drag ratio (*L*/*D*) can be simply obtained by dividing the previous two equations:

$$\frac{L}{D} = E = \frac{\cos(\gamma)}{\sin(\gamma)} = \frac{1}{\tan(\gamma)} \tag{3}$$

where γ is the flight path angle that can be obtained from the next equation:

$$\gamma = \theta - \alpha \tag{4}$$

The pitch angle (θ) is obtained from the autopilot sensors, while the angle of attack (α) is obtained from the AlphaBeta probe. A second method for glide ratio determination based on the same approach, uses a relationship of horizontal distance traveled (ΔX), vertical distance traveled (ΔZ) and flight path angle (γ) given by:

$$\tan(\gamma) = \frac{\Delta Z}{\Delta X} \tag{5}$$

By simply replacing this equality on equation 3 the second method for performance determination is obtained:

$$\frac{L}{D} = \frac{1}{\tan(\gamma)} = \frac{1}{\frac{\Delta Z}{\Delta X}} = \frac{\Delta X}{\Delta Z} \tag{6}$$

In these two previous methods, a steady-state glide is assumed where the UAV flies aligned to the relative wind in a non accelerated glide. This condition is very hard to obtain in a real world atmosphere, thus a third method based on the decomposition of the velocity vector along the three body axes (*x*, *y* and *z*) is used. This method accounts for all the oscillations that are felt in a real flight. Figure 2 illustrates the decomposition of the velocity vector in its three components (*u*, *v*, *w*). In this figure the sideslip angle is represented by β which is the angle formed between the flight path and the *x*-axis of the vehicle.

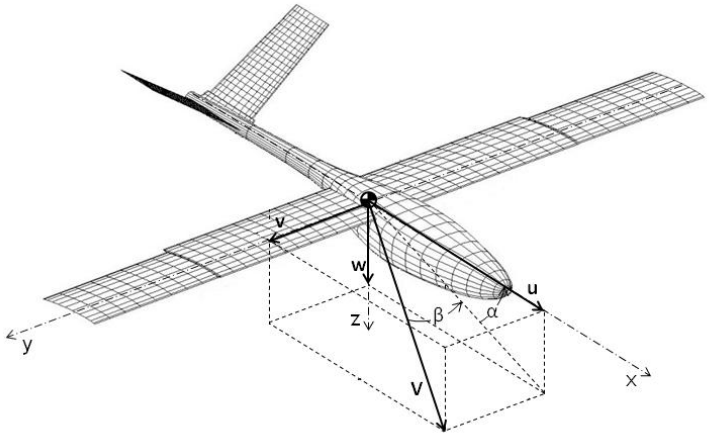

Figure 2 - Representation of the decomposition of the velocity (*V*) into its three components.

The next equations express the time derivatives of the three components of the airspeed along the vehicle axis.

$$\dot{u} = \frac{X_T - gmsin(\theta) - Dcos(\alpha) + Lsin(\alpha)}{m} + rVsin(\beta) - qVsin(\alpha)\cos(\beta) \quad (7)$$

$$\dot{v} = \frac{Y_T + gmsin(\Phi)\cos(\theta) + Y}{m} + pVsin(\alpha)\cos(\beta) - rVcos(\alpha)\cos(\beta) \quad (8)$$

$$\dot{w} = \frac{Z_T + gmcos(\Phi)\cos(\theta) - Dsin(\alpha) - Lcos(\alpha)}{m} + qVcos(\alpha)\cos(\beta) - pVsin(\beta) \quad (9)$$

In these equations X_T, Y_T and Z_T are the thrust components in the vehicle's three axes directions, which in this case are zero, because a gliding flight with the engine turned off is considered. The body angular velocities are represented by *p*, *q* and *r*, where ϕ and θ are the bank and pitch angles in earth-fixed reference frame, respectively.

These three equations are solved with respect to lift (*L*), drag (*D*) and aerodynamic lateral force (*Y*), and the lift-to-drag ratio is obtained by simply dividing *L* by *D*.

3.2. Olharapo UAV flight tests

About 32 flights aimed for performance determination were performed at the airfield of Castelo Branco. Each flight consists of a series of glides at different airspeeds that are achieved by simply changing the elevator trim position. A typical flight path for data acquisition starts with an initial climb until the UAV reaches a certain altitude followed by a power off glide flight. This cycle is repeated until the energy stored in the battery is not sufficient to perform more glides, thus proceeding to the landing stage.

During the process of data collection some difficulties relating to piloting the UAV were experienced because in most cases the wind proved to be perpendicular to the runway, making the landing maneuvers somewhat difficult. In addition, in certain situations the wind was strong and turbulent, which simply made it impossible to perform the necessary number of flight tests. Due to these limitations, it was not possible to make an acquisition of sufficient flight data to completely characterize the aerodynamic performance of the telescopic wing.

4. Results

In this chapter the results obtained for the lift-to-drag ratio for both wings are presented. The conventional wing was the first to be tested, so there are a lot more data points that clearly describe a typical efficiency curve.

Regarding the VSW, three different wingspan configurations were tested: a full wingspan configuration of 2.5m, an intermediate configuration of 2m, and a minimum wingspan configuration of 1.5m. The telescopic wing is mainly evaluated in a qualitative manner because the obtained results are limited in number.

4.1. Conventional wing results

During the flight tests with this wing installed the UAV mass was 5.6kg and the center of gravity was located at 22.2% of the wing chord. The main results obtained for the lift-to-drag ration by the three different methods as a function of airspeed are plotted in figure 3.

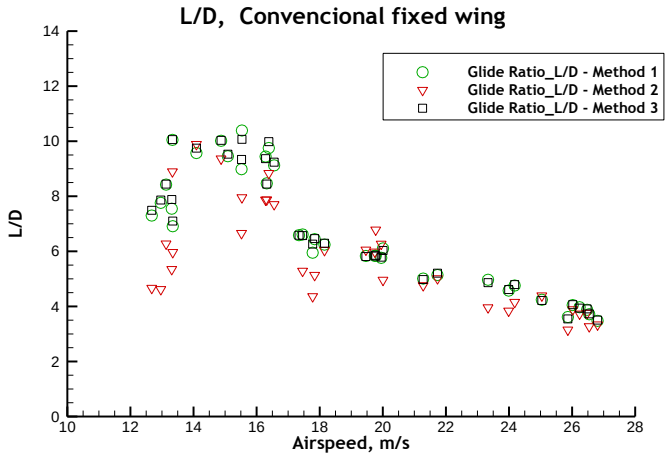

Figure 3 – Lift-to-drag ratio (*L/D*) as a function of airspeed for the conventional wing.

From figure 3 it can be seen that the three methods for performance determination produce similar results. The first and third methods show more consistency whilst method 2 present somewhat scattered results. For this wing the maximum aerodynamic efficiency is about 10, occurring at an airspeed of 15.4m/s. A minimum lift-to-drag ratio value of 3.5 was achieved for the maximum tested airspeed of 26.8m/s.

Figure 4 shows the same results as function of the lift coefficient (C_L). Only the results obtained by the first and third methods are only plotted. The glide ratio increases as the lift coefficient increases. The maximum glide ratio (10) is obtained for a lift coefficient of 0.71. On the other hand, the lowest aerodynamic efficiency occurs for the lowest lift coefficients, being the minimum approximately 3.5 for a lift coefficient of 0.2.

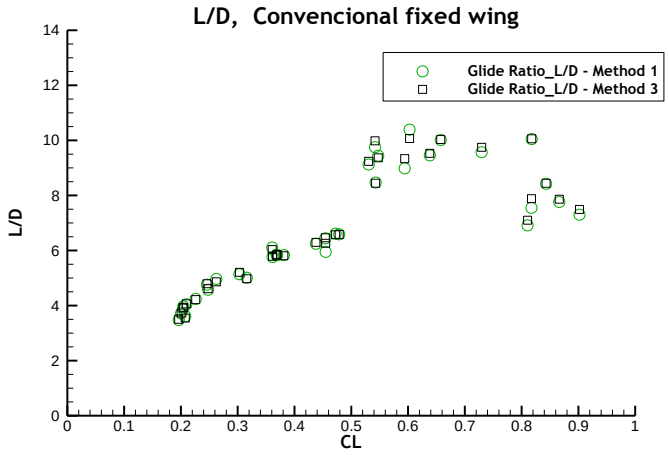

Figure 4 – Lift-to-drag ratio (*L/D*) as function of lift coefficient (C_L) for the conventional wing.

4.2. Variable span wing (VSW) results

Only the results of the lift-to-drag ratio for the position of maximum wingspan (2.5m) and intermediate wingspan (2m) are shown, since the third position, has only been tested to ascertain the behavior of the UAV in a qualitative way. During the flight tests, the UAV mass was about 1kg greater that the mass of the UAV fitted with the conventional wing, i.e. 6.65kg. The center of gravity was located at 23.7% of the wing chord.

4.2.1. Lift-to-drag ratio for maximum wingspan configuration, *b*=2.5m

Figure 5 shows the results for the lift-to-drag ratio as a function of airspeed for the VSW with a wingspan configuration of b=2.5m. For this wingspan configuration, the three calculation methods yield results that are somewhat scattered. In the same way as for the conventional wing, methods 1 and 3 present more consistent results. It is possible to detect a high density of efficiency points for an airspeed of about 15.7m/s, where the lift-to-drag ratio approaches 8.5. The lowest lift-to-drag ratio, 6.6, was obtained for the maximum tested airspeed of 21m/s. Compared with the conventional wing, this wing always presents lower values of lift-to-drag ratio. These results may be explained by the fact that the telescopic wing airfoil is not as efficient as the conventional wing, as well as the existence of a discontinuity between the IFW and the OMW, which makes interference and induced drag increase.

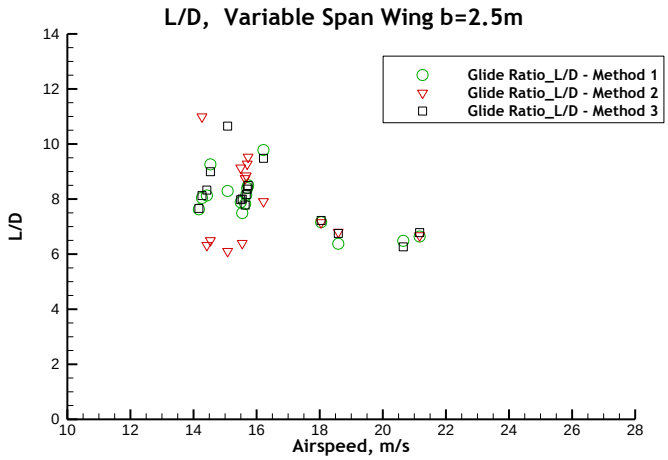

Figure 5 – Lift-to-drag ratio (*L*/*D*) as function of airspeed for the telescopic wing with *b*=2.5m.

In figure 6 the results obtained by method 1 and 3 for the lift-to-drag ratio as functions of lift coefficient are plotted. As expected, the lift-to-drag ratio increases with increasing lift coefficient. The highest density of efficiency points occurs at a lift coefficient of 0.67 where the lift-to-drag ratio is about 8.5.

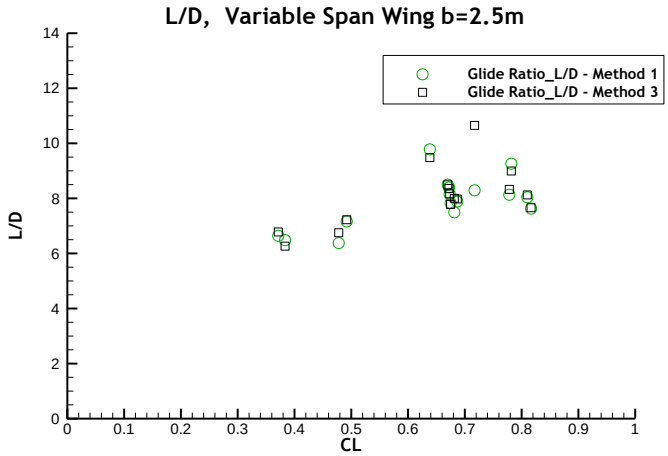

Figure 6 - Lift-to-drag ratio (*L*/*D*) as function of lift coefficient (C_L) for the telescopic wing with *b*=2.5m.

4.2.2. Lift-to-drag ratio for an intermediate wingspan configuration, *b*=2m

Figure 7 shows the results for the lift-to-drag ratio as a function of airspeed for the VSW with an intermediate wingspan configuration of *b*=2m. For this configuration, despite the scattered results, it is possible to identify an area of greater concentration of points for an airspeed of approximately 16.6m/s, where the three methods converge to an aerodynamic efficiency

around 8. With the increase of airspeed, the lift-to-drag ratio decreases, reaching a minimum of 4.7 at 25.7m/s.

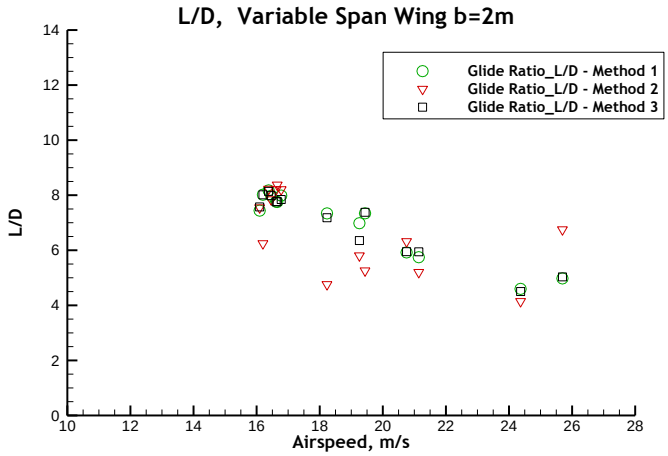

Figure 7 – Lift-to-drag ratio (*L/D*) as function of airspeed for the telescopic wing with *b*=2m.

Comparing these results with the results obtained for the conventional wing, it appears that for 26m/s, the aerodynamic efficiency of the telescopic wing in its intermediate configuration (*b*=2m) presents a value that tends toward 4.7, which is higher than that of the conventional wing which is close to 3.5. These results are in agreement with the numeric results [14] that predicted that the aerodynamic efficiency of the VSW would surpass that of the conventional wing at airspeeds greater than 22.5 m/s. In figure 8, the same results are plotted as function of the lift coefficient.

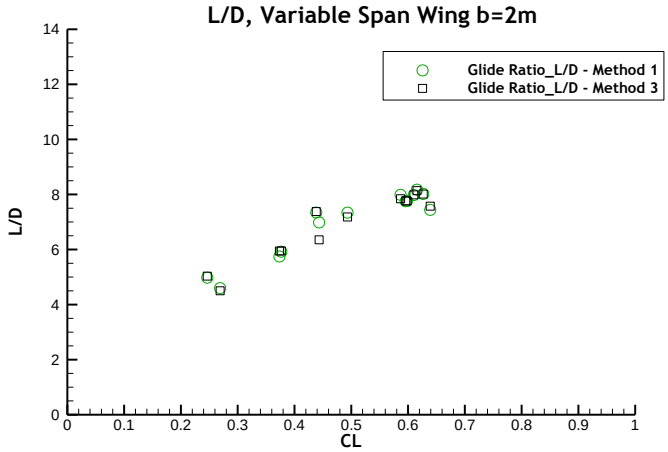

Figure 8 - Lift-to-drag ratio (*L/D*) as function of lift coefficient (C_L) for the telescopic wing with b=2m.

In the same way as the telescopic wing in its maximum wingspan configuration, the lift-to-drag ratio increases with the increase of the lift coefficient, peaking at 8 for a lift coefficient equal to 0.62. The minimum lift-to-drag ratio of 4.7 was obtained for a lift coefficient of 0.26.

Analyzing the results of lift-to-drag ratio as a function of lift coefficient for the UAV with the conventional wing and with the telescopic wing fitted, it appears that for the same lift coefficient, the VSW shows lift-to-drag ratio values always below the conventional wing. However, for the variable span wing in an intermediate configuration of 2m, the glide ratio gets very close to those of the conventional wing, at a lift coefficient equal to 0.27. This may indicate that, at a certain lift coefficient, the aerodynamic efficiency of the VSW can surpass that of the conventional fixed wing. In order to fully characterize the UAV aerodynamic

performance with the VSW, more flight tests should be conducted particularly at low lift coefficients.

4.2.3. Flight handling qualities

The telescopic wing allows not only varying the wingspan symmetrically to adjust to different flight conditions but it can also be actuated asymmetrically thus allowing to carry out roll control maneuvers.

From the three wingspan configurations that were tested (2.5m, 1.5m and 2m), it was found that the lower the total wingspan was the greater the airspeed reached. It was also observed that during the transitions between different configurations of wingspan, the speed did not undergo abrupt changes. Instead, trimmed flight was reached gradually.

This wing demonstrated great ability in performing roll maneuvers throughout asymmetrical wings extension, where no undesirable behavior was felt by the pilot. The asymmetric wing deployment was performed by the pilot as in a conventional wing which uses ailerons to perform this maneuver. The only difference was experienced in roll rate that for a given input was lower with telescopic wing, thus making the roll response slower than the conventional wing. This can easily be overcome, by adjusting the wing extension to the control input, thus making the response approach the conventional wing with ailerons.

5. Concluding remarks

This work was developed to determine the aerodynamic performance of the Olharapo UAV fitted with two different wings: a conventional fixed wing and a variable span morphing wing. An analysis of the flight mechanics of the UAV in the condition of gliding flight was performed, from which three different approaches were established to determine the lift-to-drag ratio. For the conventional fixed wing, a well defined efficiency curve was obtained, where the maximum lift-to-drag ratio was about 10 at a airspeed of 15.4m/s. Regarding the VSW, three different wingspan configurations were tested: a full wingspan configuration of 2.5m, an intermediate configuration of 2m, and a minimum wingspan configuration of 1.5m. Although there were not sufficient data that could completely characterize the efficiency curve for the VSW, two major clusters of efficiency points were observed. For the full wingspan configuration, a lift-to-drag ratio of 8.5 was obtained at an airspeed of 15.7 m/s and a C_L of 0.67. Concerning the intermediate wingspan configuration, it was possible to perceive that for low lift coefficients, the lift-to-drag ratio tends to the same values obtained for the UAV with the conventional wing. This may indicate that at a certain speed, the aerodynamic efficiency of the VSW can surpass that of the conventional fixed wing. In order to fully characterize the UAV aerodynamic performance with the VSW, more flight tests should be conducted particularly at low lift coefficients.

References

[1] Tidwell Z., Joshi S., Crossley W., and Ramakrishnan S., "Comparison of Morphing Wing Strategies Based Upon Aircraft Performance Impacts", AIAA Paper 2004-1722, *45th AIAA/ASME/ASCE/AHS/ASC Structures, Structural Dynamics and Materials Conference*, Palm Springs, California, 19-22 April, 2004

[2] A. F. Stuttgart, "TF - Teleskop-Flügel," 2013. [Online]. Available: http://www.uni-stuttgart.de/akaflieg/en/projects/all-fs-projects/fs-29-tf.html. [Accessed: 18-Jul-2013].

[3] I. Gevers Aircraft, "Gevers Aircraft, Inc. Genesis." [Online]. Available: http://www.geversaircraft.com/. [Accessed: 03-Aug-2013].

[4] L. Arrison, K. Birocco, C. Gaylord, B. Herndon, K. Manion, and M. Metheny, "2002-2003 AE/ME Morphing Wing Design," Blacksburg, Virginia, 2003.

[5] D. Malewicki, "Aerovisions Inc. , UMAAV," 2004. [Online]. Available: http://www.canosoarus.com/05UMAAV/UMAAV01.htm. [Accessed: 20-Jan-2014].

[6] J. Blondeau, "Development and testing of a Variable Aspect Ratio Wing using Pneumatic Telescopic Spars", MSc, University of Maryland, College Park , USA, 2004.

[7] J. Blondeau and D. Pines, "Design na Testing of a Pneumatic Telescopic wing for Unmanned Aerial Vehicles," *Journal of Aircraft*, no. 44, pp. 1088–1099, 2007.

[8] J.S. Bae, T. M. Seigler, and D. J. Inman, “Aerodynamic and Static Aeroelastic Characteristics of a Variable-Span Morphing Wing,” *Journal of Aircraft*, vol. 42, no. 2, pp. 528–534, Mar. 2005.
[9] R. D. Vocke, C. S. Kothera, B. K. S. Woods, E. A. Bubert, and N. M. Wereley, “One Dimensional Morphing Structures for Advanced Aircraft,” in *Recent Advances In Aircraft Technology*, R. K.Agarwal, Ed. Intech, 2012.
[10] R. M. Ajaj, M. I. Friswell, E. I. S. Flores, and O. Little, “Span Morphing: A Conceptual Design Study” in *Proceedings of AIAA/ASME/AHS Adaptive Structures Conference*, Honolulu, USA, 2012, AIAA, pp. 1–12.
[11] M. Stern and E. Cohen, “VAST AUAV (Variable AirSpeed Telescoping Additive Unmanned Air Vehicle),” Lexington, 2013.
[12] Graeme, “The Makhonine telescopic wing,” 2007. [Online]. Available: http://www.ww2aircraft.net/forum/other-mechanical-systems-tech/makhonine-telescoping-wing-8527.html. [Accessed: 16-Jan-2014].
[13] S. Barbarino, O. Bilgen, R. M. Ajaj, M. I. Friswell, and D. J. Inman, “A Review of Morphing Aircraft”, *Journal of Intelligent Material Systems and Structures*, vol. 22, no. 9, pp. 823–877, 2011.
[14] Mestrinho J., Gamboa P., Santos P.D., Design Optimization of a Variable-Span Morphing Wing for a Small UAV. 52th AIAA/ASME/ASCE/AHS/ASC Structures, Structural Dynamics and Materials Conference, Denver, Colorado, 4-7 April, 2011.
[15] Tavares F.M., Roll Motion Control of a Dissymmetrical Wingspan Aircraft, MSc Thesis, Departamento de Ciências Aeroespaciais, Universidade da Beira Interior, Covilhã, October 2011.
[16] Felício J., Santos P.D., Gamboa P., Silvestre M.A., Evaluation of a Variable-Span Morphing Wing for a Small UAV. 52th AIAA/ASME/ASCE/AHS/ASC Structures, Structural Dynamics and Materials Conference, Denver, Colorado, 4-7 April, 2011.
[17] Santos P.D., Gamboa P., Santos P.M., Silva J.M.,. Structural Design of a Composite Variable-Span Wing. 4th International Conference on Integrity, Reliability and Failure, Funchal, 23-27 June 2013.
[18] Gamboa P., Santos P.D., Silva J.M., Santos P.M., Flutter Analysis of a Composite Variable-Span Wing. 4th International Conference on Integrity, Reliability and Failure, Funchal, 23-27 June 2013.
[19] Sousa, J., Santos, P.D., Gamboa, P., Control Systems for UAV Flight Testing, International Conference on Engineering ICEUBI2013 – Engineering for Economic Development, Covilhã, Portugal, 27-29 November, 2013.